Integrated Modeling of the Ultrasonic/Sonic Drill/Corer - Procedure and Analysis Results

Mircea Badescu, Xiaoqi Bao, Yoseph Bar-Cohen, Zensheu Chang, Stewart Sherrit

JPL/Caltech, (MS 67-119), 4800 Oak Grove Drive, Pasadena, CA 91109-8099,

ABSTRACT

Rock and soil penetration by coring, drilling or abrading is of great importance for a large number of space and earth applications. An Ultrasonic/Sonic Drill/Corer (USDC) has been developed as an adaptable tool for many of these applications [Bar-Cohen et al, 2001]. The USDC uses a novel drive mechanism to transform the ultrasonic or vibrations of the tip of a horn into a sonic hammering of a drill bit through an intermediate free-flying mass. As the pace of adapting the USDC to various applications has increased, it has become more critical to develop a efficient simulation tool to predict the performance of various designs. A series of computer programs that model the function and performance of the USDC device were previously developed and tested against experimental data [Bao et al, 2003]. The combination of these programs into an integrated modeling package and the analysis of simulated results will be described in this paper.

Keywords: Ultrasonic horn, ultrasonic drilling, soil drill, piezoelectric devices.

1. INTRODUCTION

Future NASA exploration missions to Mars, Europa, Titan, comets and asteroids are seeking to perform sampling, in-situ analysis and possibly the return of material to Earth for further tests. Existing drilling techniques are limited by the need for large axial forces and holding torques, high power consumption and an inability to efficiently duty cycle. Lightweight robots and rovers have difficulties accommodating these requirements. To address these key challenges to the NASA objective of planetary in-situ rock sampling and analysis, an ultrasonic/sonic driller/corer (USDC) was developed [Bar-Cohen et al, 2001; Sherrit et al, 2000].

Figure 1 - USDC drilling

The actuator of the USDC is an ultrasonic horn transducer that is driven by a piezoelectric stack. Unlike the typical ultrasonic drill where the drill stem is acoustically coupled to the transducer, the horn transducer in the USDC drives a free flying mass (free-mass), which bounces between the horn tip and a drill stem at sonic frequencies. The impacts of the free-mass create stress pulses that propagate to the interface of the stem tip and the rock. The rock fractures when its ultimate strain is exceeded at the rock/bit interface. This novel drilling mechanism has been shown to be more efficient and versatile than conventional ultrasonic drills under a variety of conditions. The low mass of a USDC device and the ability to operate with minimum axial load with near zero holding torque (see Fig. 1) offers an important tool for sample

Mircea.Badescu@jpl.nasa.gov, Phone 818-393-5700, Fax 818-393-4057, http://ndeaa.jpl.nasa.gov

acquisition and in-situ analysis. Another important characteristic of the USDC is the capability to operate in the restrictive space environment.

The functionality of the USDC was modeled to predict its performance. The developed model describes five elements involved in the drilling i.e. the electrical driver, ultrasonic transducer, free-mass, drill stem, and the rock. In a previous publication the main elements and the interaction between them were analyzed and modeled separately [Bao et.al. 2003]. A one-dimensional model was then developed for each interaction and an integrated software program was developed to simulate the operation of all parts of the USDC. The time to run the individual components and the integrated modeling ranged from days up to a week depending on the design. In addition user input was required at many points in the calculation. The lack of autonomy and the lengthy calculation times forced us to develop an integrated package to run automatically, without human intervention, and in a shorter period of time. These component programs run in ANSYS^{TM} or MATLAB^{TM} and require input files and transfer of information from one component program to the next. Separate programs were developed to generate these input files, provide design parameters, read output files of the main component programs and extract useful information for the next programs. All these component programs and the new auxiliary programs are controlled by a UNIX script and can run automatically. This paper presents the modeling program package and the analysis results for a specific USDC application.

2. MODELING. COMPONENT PROGRAMS

The USDC device consists of three main parts: an ultrasonic transducer (piezoelectric stack, a backing element, and a horn), a free-mass, and a drill stem. Fig. 2 shows a schematic of the USDC device. The ultrasonic/sonic transducer can be designed to vibrate at a frequency from 5 to 25kHz depending on the application. The vibrations of the horn tip excite the free-mass, causing it to bounce between the horn tip and the top of the drill stem with an average frequencies in the range of 100 to 1000 Hz. The free-mass transfers energy from the ultrasonic transducer to the drill stem. The shock waves caused by the impacts of the free-mass on the drill bit propagate to the bit/rock interface and wherever the rock is strained past its ultimate strain it fractures. In order to determine the critical issues related to the control and optimization of the drill, models of the interaction at the various interfaces of the drill were investigated. The four interactions that were modeled include: 1) transducer with the driving circuit, 2) horn tip with the free-mass, 3) free-mass with the drill stem and 4) base of the drill stem (bit) with the rock. The component programs were presented in detail in a previous paper [Bao et al, 2003]. The following is a brief description of these programs and the combination in an integrated simulation that can run automatically. To date, only the first three components have been integrated into the package. The integrated package was used to analyze various designs of a USDC device for ice coring, and the results are presented in this paper.
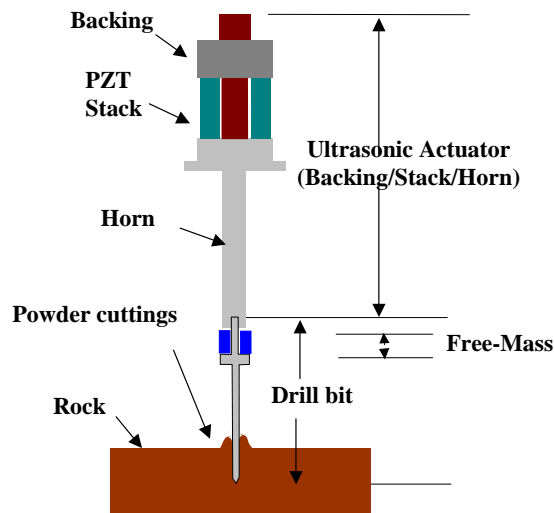

Figure 2 - USDC schematics

2.1. Transducer/ ultrasonic actuator

The transducer/ultrasonic actuator consists of a PZT-8 stack maintained in compression between a horn and a backing by a pre-stress bolt. The horn amplifies the vibration amplitude by varying the cross-sectional along its length. Various shapes of the horn were analyzed, including a dog-bone horn, a solid horn and a stepped horn. The transducer is a composite longitudinal vibrator with varying cross sections and can be modeled by the Mason equivalent circuit as presented in a previous paper [Sherrit et al, 1999]. In order to include engineering details in the final transducer design the finite element approach was used to determine the full frequency response of this piezoelectric device. An electromechanically coupled element [Allik and Hughes, 1970] was applied to model the piezoelectric material, which is available in commercial software ANSYS^{TM}.

In this high power ultrasonic application, the transducer is designed and fabricated to have high mechanical Q, and is operated at or near its first longitudinal resonance frequency. Using modal analysis allowed us to isolate and concentrate on this resonance mode and it simplifies the model and reduces the computing time. Solving the generalized eigenvalue problem of finite element equations, the resonance frequencies and corresponding mode shapes can be found. We obtain a set of resonance frequencies, $\omega_1, \omega_2, \ldots, \omega_n$ and normalized mode shapes (eigenvectors)

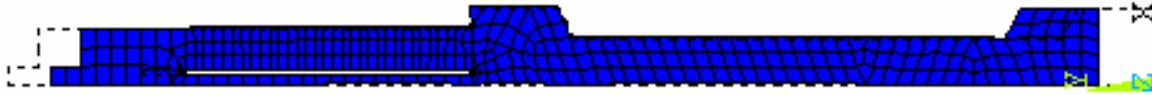$$\{\xi_1\}, \{\xi_2\}, \ldots, \{\xi_n\}. \tag{1}$$

Figure 3 - Mode shape

Fig. 3 shows the modal shape of the first nonzero-frequency resonance of the transducer calculated by ANSYS^{TM}. The mode is basically a longitudinal vibration with larger displacement at the horn tip (right hand side in Fig. 3) than at the back. The calculated resonance frequency was found to be 5.275 kHz using the material property data provided by the manufacturers, which was very close to the measured resonance frequency located between 5.2 to 5.3 kHz.

By expressing the displacement as the summation of the modal shapes as:

$$\{\xi\} = \sum_n d_i \{\xi_i\}. \tag{2}$$

The finite equations can be converted to modal equations and be simplified to an equivalent circuit for convenience in computation as was reported in a previous work [Bao et al, 2003],

$$(\omega_i^2 + j\omega R_i - \omega^2)d_i = p_i V + Fm_i$$

$$Q = \sum_n p_i d_i + C_0 V \qquad \qquad i=1,\ldots n \tag{3}$$

where d_i is the amplitude of the mode i, Q is the electric charge on the electrode, R_i, p_i and F_{mi} are effective damping, electromechanical coupling and force for the modes respectively. The R_i and p_i can be calculated from the finite element matrixes, and F_{mi} is expressed as

$$Fm_i = \{\xi_i\}^T \{F\}, \tag{4}$$

where $\{F\}$ is the vector of the force applied on the nodes.

Only the first longitudinal mode is taken into account in the analysis. With these substitutions (3) becomes:

$$(\omega_1^2 + j\omega R - \omega^2)d = pV + Fm$$

$$Q = pd + C_0 V \tag{5}$$

where subscripts are omitted for simplification.

A further simplification is shown for (5) by representing the response of the device by an equivalent circuit around resonance as is shown in Fig. 4, where subscripts m are added to denote that the symbols actually represent mechanical variables and parameters. The element in the dashed square is the sketch of the electric driving circuit.

Upon inspection we have $L_m = 1$, $C_m = 1/\omega_i^2$ and the mechanical "current" I_m is the modal velocity

$$I_m = \dot{d}. \tag{6}$$

When the transducer is driven electrically and is mechanically unconstrained (no impacts with the free-mass), the modal velocity can be shown to be

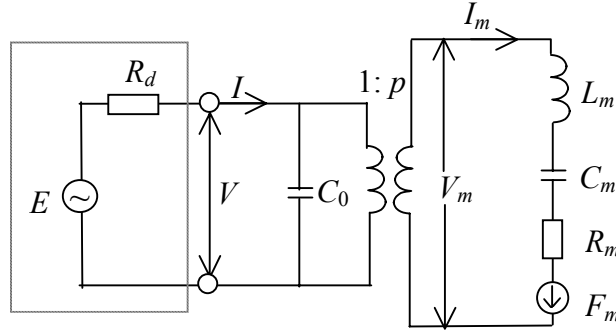$$I_m = \frac{pV}{j(\omega L_m - \frac{1}{\omega C_m}) + R_m}.$$ (7)

Figure 4 - Schematic of the equivalent circuit of the transducer around resonance. The generator source is also included in the dashed square.

2.1.1. Reaction of free-mass impacts to the transducer

In the operation of the USDC, a small preload force, either from gravity or from a spring is applied to the transducer to close the gap between the horn tip and the free mass. The force pushes the transducer down toward the free-mass and the bit. A harmonic voltage at a frequency around the resonance drives the transducer. The free-mass, energized by the impacts with the vibrating horn tip, then, bounces between the bit and horn tip and maintains a gap between them. The impacts of the free-mass to the horn tip affect both vibration and translation movements of the horn transducer.

a) Translation movement of the horn transducer
We assume the preload force is constant and produces an acceleration a of the transducer. Suppose an impact happens at time t_I, and contact time is very short, the contact force can be expressed as

$$F_c = f_I \delta(t - t_I)$$ (8)

where δ is the delta function. Using momentum conservation in the impact, we have

$$f_I = -m\Delta v_I$$ (9)

where m and Δv_I is the mass and velocity of the free-mass respectively. Each impact results in a change of the center of mass (COM) velocity of the horn by

$$\Delta U_I = \frac{-m\Delta v_I}{M} H(t - t_I)$$ (10)

where M is the total mass of the horn transducer, and H is the step function. Therefore, the COM velocity of the transducer becomes

$$U = U_0 + at + \sum_I \Delta U_I$$ (11)

The displacement of the transducer is therefore the time integral of the velocity.

b) Vibration of the transducer with constant harmonic voltage driving
When the source resistance R_d, as shown in Fig. 3, is zero the transducer is driven by a constant voltage. In this case, the vibration of the transducer can be solved explicitly. From the equivalent circuit, we can write the corresponding differential equation as

$$L_m \ddot{d} + R_m \dot{d} + C_m d = pV + F_m$$ (12)

The solution of this equation is the summation of the vibration induced by the electric voltage V and the vibration caused by the mechanical force F_m. The steady solution for a harmonic voltage $V = V_0 \exp(j\omega t)$ is

$$I_{me} = \dot{d}_e = \frac{pV}{j(\omega L_m - 1/\omega C_m) + R_m} \tag{13}$$

A mechanical force is caused by the impacts of the free-mass on the horn tip and can be determined from (4), (8) and (9), to be

$$F_m = \xi_t f\delta(t - t_I) = -m\Delta v_I \xi_t \delta(t - t_I) \tag{14}$$

where ξ_t is the tip displacement of the mode shape. The solution of (12) for the impact force Fm is a free ring-down vibration after the impact time t_I and is expressed as

$$I_{mI} = \dot{d}_I = -\frac{m\Delta v_I \xi_t}{L_m} \exp[(-\alpha + j\omega_f)(t - t_I)] \tag{15}$$

where α is the damping coefficient and ω_f is the free vibration frequency, and

$$\alpha = -\frac{R_m}{2L_m} \tag{16}$$

$$\omega_f = \sqrt{\omega_1^2 - (R_m/2L_m)^2} \tag{17}$$

The final solution of the modal velocity is

$$I_m = \dot{d} = \dot{d}_e + \sum_I \dot{d}_I = I_{me} + \sum_I I_{mI} \tag{18}$$

c) Transducer driven by a driver with output resistance

In general, the output resistance of electronic drivers is not zero. The resistance will reduce the output voltage, increase energy loss and change the characteristics of the vibrations induced by the impacts.

The same approach utilized in the previous section can be applied to the case of non-zero output impedances of the drive circuit except resulting more complicated solution. The steady solution of the electric driving voltage in this case is then

$$I_{me} = \dot{d}_e = \frac{pEZ_x/(R_d + Z_x)}{j(\omega L_m - 1/\omega C_m) + R_m} \tag{19}$$

where the impedance of the transducer Z_x is

$$Z_x = \frac{j(\omega L_m - 1/\omega C_m) + R_m}{j\omega C_0[j(\omega L_m - 1/\omega C_m) + R_m] + 1/p^2} \tag{20}$$

The solution for the impact is

$$I_{mI} = \dot{d}_I = -\frac{m\Delta v \xi_t}{L_m} \exp[S(t - t_I)] \tag{21}$$

where S is the solution of

$$L_m C_m R_d C_0 S^3 + (L_m C_m + R_m C_m R_d C_0)S^2$$
$$+ (R_m C_m + p^2 R_d C_m + R_d C_0)S + 1 = 0 \tag{22}$$

This cubic equation has one real root and a pair of conjugate complex roots. For the free attenuating vibration, the solution S is in the form as

$$S = -\alpha + j\omega_f. \tag{23}$$

Although it is possible to obtain explicit expression of the solution, the expression is cumbersome and not accurate in practical numerical calculations.

d) Interaction between the transducer and the electric driver

Power output from the voltage source P_E is the time averaged integral of product of multiplication of the source voltage by the current and is expressed as

$$P_E = \frac{1}{T}\int_T E(t)I(t)dt$$

$$= \frac{1}{T}\int_T E(t)I_e(t)dt + \frac{1}{T}\int_T E(t)\sum_I I_I(t)dt \qquad (24)$$

or

$$P_E = P_{Ee} + P_{EI}, \qquad (25)$$

where the first item in (24), P_{Ee}, is the power with no free-mass loading and   is the power change introduced by the free-mass loading. $I_e(t)$ is the current though the source due to the electric drive voltage, and $I_I(t)$ is the current due to the free-mass impacts,

$$I_e(t) = \text{Re}(\frac{E}{Z_x(\omega) + R_d}) \qquad (26)$$

$$I_I(t) = \text{Re}(\frac{pI_{mI}}{j\omega_f C_0 R_d + 1}). \qquad (27)$$

The power lost on the resistor P_d is calculated using the time-averaged power

$$P_d = \frac{1}{T}\int_T R_d[I(t)]^2 dt = \frac{R_d}{T}\int_T [I_e(t) + \sum_I I_I(t)]^2 dt \qquad (28)$$

It should be noted that, in these power calculations, all voltages and currents are expressed as real functions of time rather than their complex expression. Beside, the currents introduced by the impacts $I_I(t)$ attenuate with time and oscillate at the frequency ω_f, which may be different from the driving frequency ω. Therefore, the integrals in (24) and (28) are in a general form of

$$Int = \int \cos(at + f)\cos(bt + g)e^{-ct}dt. \qquad (29)$$

2.2. Horn tip – free mass impact

The horn tip – free-mass impacts have been modeled in two different approaches.

In the first approach, a simple collision model was applied to explore the basic mechanism of the horn/free-mass driving. In this model, we assume that the energy loss and time duration of the impact is negligible, and the mass of the horn is much larger than the free-mass.

A computer simulation routine, which traces the position of the free-mass until it leaves the tip vibration range, was programmed. The routine calculates the free-mass speed after interaction with the horn. The final speed of the free-mass vary with respect to the vibration phase and the value of the initial speed. The model accounts for multiple impacts that become possible when the impact is timed appropriately. Although it is possible that speed after interaction may be less than the initial speed when the tip velocity is negative, the computed results show that the free-mass final velocity increases on average after interaction with the vibrating horn tip.

In the second approach a finite element analysis of the impact was performed. The assumption that the horn mass is much greater than the free-mass in the simple collision model, is true if we include the total mass of the horn transducer. However, in the short time duration that the impact lasts, the impact wave propagates to a limited range within the horn transducer. The remaining part of the transducer is actually not involved in the impact. So, the assumption of a horn mass much greater than the free-mass may not be correct. To explore the details of the real impact/driving process, a finite element model was constructed.

In the model, the horn transducer is truncated to a λ/4 long bar. A symmetric boundary condition is applied at the other end of the bar. The validity of this truncation is based on the fact that the structure difference in the area far from the

point of impact will not make a difference to the free-mass bouncing process. From the viewpoint of wave propagation the free-mass should not "feel" the structure difference in the area, as long as the free-mass leaves the tip surface before the impact wave can propagate through the medium and be reflected back to the impact spot. Axisymmetrical solid elements are used to represent the horn tip. The initial conditions, i.e. the displacements and velocities of the nodes, are set to typical longitudinal vibration values in the bar. Compression only link elements are placed between the nodes on the surfaces of the free-mass and the horn tip in the contact area. The free-mass is treated as a rigid block with a curvature in the contact area.

The finite element approach provides a more accurate description of the free-mass speed after the collision and the time duration of the collision. Comparing with the simple collision model, the maximum speed is typically lower for the finite element approach than that obtained from the simple collision model. This implies a limited effective mass of the horn. The finite element approach explored two phenomena that were not accounted for in simple collision model, elasticity of the horn and the effective mass involved in the impacts. Based on the phenomena, a spring-mass model was developed. The model uses a mass and two springs to present the horn as shown in Fig. 5.

The parameters of the mass M and front spring k are determined using the rebound velocity and contact time obtained by the finite element approach. The top spring constant K is set by the resonance frequency of the horn transducer. The results are found to agree exceptionally well with the finite element results. The spring-mass model therefore provides a more time efficient solution with reasonable accuracy, which was required by the integrated simulation program. This approach was used in the final modeling of the USDC.
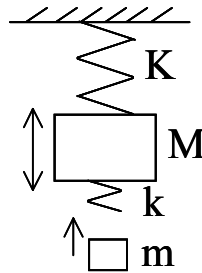

Figure 5 - The spring-mass collision model

2.3. Free mass – drill stem impact

The engineering model of the drill stem consists of a head and a thin cylindrical bar. The free-mass impacts the head and creates a stress wave that propagates toward the lower end of the bit. A finite element model, which is similar to that used for horn tip and free-mass interaction, was utilized to investigate the impacts. The length of the drill stem was fixed and chosen to be long enough to avoid the interference from the reflected wave of the bottom.

2.4. Simplified computer program

A computer program was developed to simulate the operation of the drill system including the horn transducer, free-mass, drill stem and the electric driver. The program was able to predict the performance of the USDC under a variety of initial conditions.

In the simulation, we assumed that the vibrations in the drill bit induced by the previous free-mass impacts were attenuated when the free-mass returns and hits the drill stem. We also neglected the movement of the drill stem with respect to the rock, since it is very slow in comparison to the quick motion of the free-mass. Therefore the top surface of the drill stem is set at the same position for the each of the impacts. Experimental observations suggest that this is a valid assumption. Replay of the video record taken by a high-speed camera showed the motion of the upper end of the drill stem was very small compared with the motion of the free-mass or the transducer's horn tip.

The flowchart of the calculation procedure is presented in Fig. 15. We start the simulation by setting the initial values of the position and velocity of the horn and the free-mass. The software traces the translation movements of the horn transducer and the free-mass as well as the vibration of the horn as functions of time. It predicts the time and location of the free-mass/horn or free-mass/bit collision. Using the data of the free-mass/horn and free-mass/bit impacts that were determined from the models mentioned in previous paragraphs, the simulation calculates the changes of the variables as time evolves. The movements and vibration due to the impact are recorded along with the impact momentum and time.

The program then proceeds to determine the next impact. The energy supplied by the electric source and delivered to the transducer is integrated and recorded concurrently. The statistics reported by the program include; electric input power, mechanical output power delivered to the drill stem, average and distribution of the free-mass speed, etc. The first 20% of the events are excluded in order to eliminate the possible influence of the initial settings.

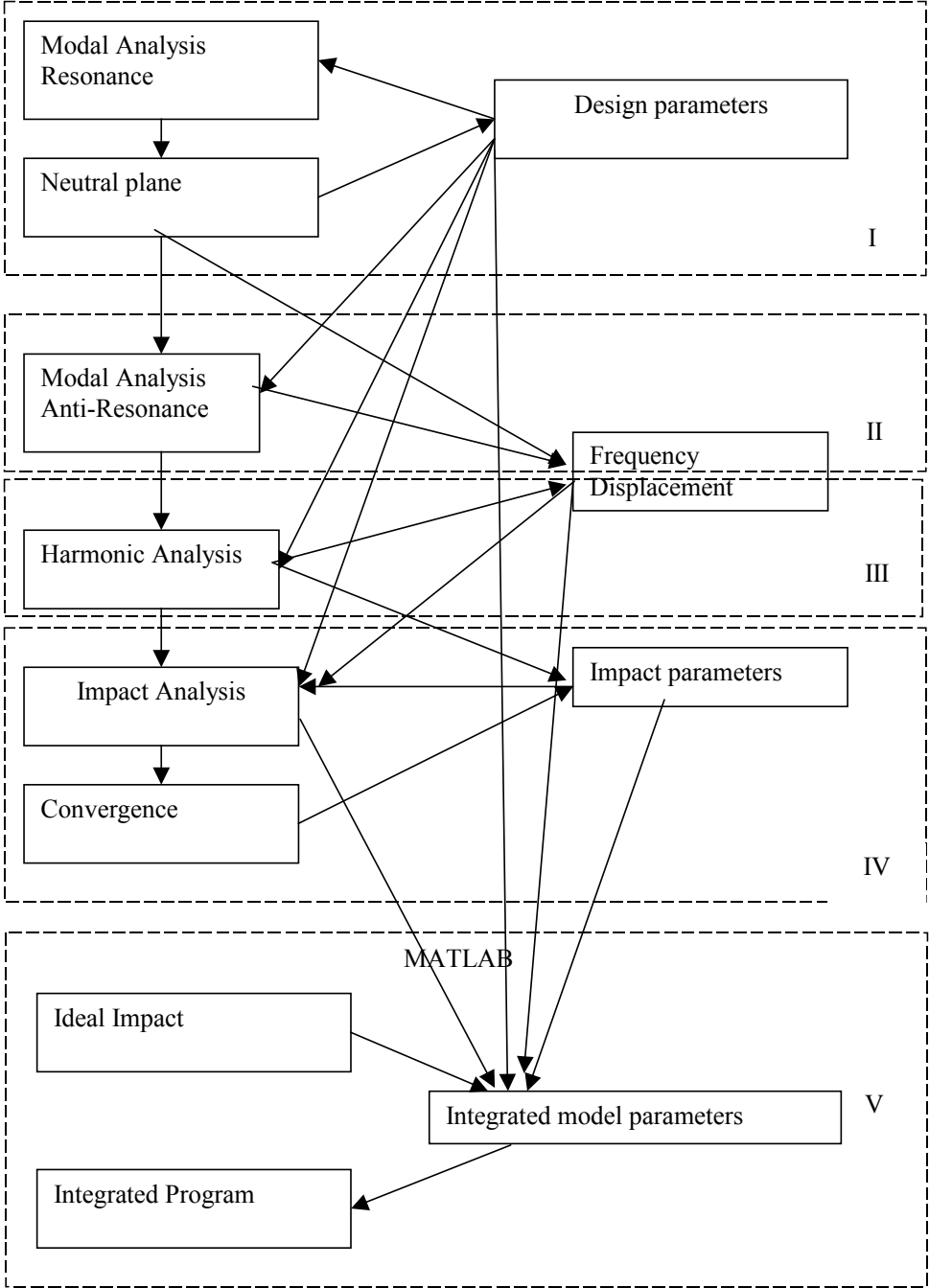## 3. MODELING. INTEGRATED PROGRAM PACKAGE

Figure 6 - Integrated program package diagram

The schematic diagram of the integrated program package is shown in Fig. 6. ANSYS^{TM} and MATLAB^{TM} are used to run the component analysis programs. Preparation of input files, reading and analysis of output files, and preparation of data files are done by C++ programs. The flow of the whole program package is controlled by a UNIX script.

The first section of the program package determines the resonance frequency of the transducer and the relative displacements of key points of the transducer. A C++ program prepares the input file for ANSYS^{TM} using data from a design parameters file. After the modal analysis is done the results are read by another C program and the relative displacement of the mounting point is compared with a predefined value. If the relative displacement of the mounting point is above a desired value, the design parameters file is modified in order to reduce the mounting point displacement. The modal analysis loop is then restarted and repeated until the displacement of the mounting point is below the specified limit. In order to reduce the computation time the iterations are done with a low resolution finite element mesh and then the final cycle is re-executed with a higher resolution finite element mesh.

Once the design parameters are finally fixed the resolution is set for all the following ANSYS^{TM} component programs.

Second section is the modal analysis – anti-resonance. The input file for the ANSYS^{TM} is generated by a C++ program. The design parameters and the mesh resolution are read from the design parameters file. The modal analysis - anti-resonance is run in ANSYS^{TM}, the output is saved in a file and is read and the important information extracted by another C++ program.

The subsequent section is the harmonic analysis which calculates the tip displacement. A C++ program reads the design parameters and the mesh resolution from the design parameters file and generates the input file for the ANSYS^{TM}. The frequency interval of the harmonic analysis is determined from modal analysis. The harmonic analysis is run in ANSYS^{TM} and the output is saved in a file. This file is then read and the important information extracted by another C++ program.

The next section performs the impact analysis of the free mass with the vibrating horn tip. A C++ routine prepares the input ANSYS^{TM} file using design parameters file and vibration amplitude and frequency provided by previous analysis. The ANSYS^{TM} generates the displacements of the horn tip and free mass nodes involved in impact. From these results a C++ program determines the final velocity of the free mass after the impact. The iterations are run for the impact occurring at various phase moments of the tip vibration.

The following sections are run in MATLAB^{TM}. The first MATLAB^{TM} script simulates the ideal impact between the free mass and the horn tip and the final velocity of the free mass after the impact is determined. The results of this simulation are compared with the results of the finite element run in ANSYS^{TM} to determine the parameters used in the final integrated MATLAB^{TM} simulation. One of the outputs generated by the integrated simulation is the power transmitted to the drill bit. It can be provided as the total power transmitted to the bit or the total power transmitted to the bit by impacts for which the free mass has a momentum higher that a predefined value. The predefined momentum value is determined by the drilling medium and drill cutting geometry.

The program package can be further included in an optimal design algorithm, like the Genetic Algorithm or other optimization techniques.

4. ANALYSIS RESULTS

The USDC application chosen to illustrate the integrated modeling is a gopher that has to drill 20m deep ice [Bar-Cohen et al, 2004]. Three types of design were considered for analysis as shown in Fig. 7: a solid horn (Fig. 7,c), a stepped horn (Fig. 7,d), and a "dog-bone" horn. For the "dog-bone" type design four different designs were analyzed: equal base and head (Fig. 7,b), longer base (Fig. 7,a), longer head (Fig. 7,f), and thinner neck (Fig. 7,e). For all these designs the PZT stack, the backing, and the stress bolt were identical. In the modal analysis - resonance loop the horn neck length was modified such that the displacement of the mounting plane is close to zero. For all designs the mounting plane was chosen to be the plane that separates the PZT stack from the horn base.

Fig. 8 shows the design of the transducer with "dog-bone" horn. Since the PZT stack, backing, stress bolt, and neutral plane are identical for all designs the resonance frequency is kept constant for all designs. The modal analysis of the designs showed that the cross-sectional area of the horn, the length of the horn base and head determine the total length of the horn.
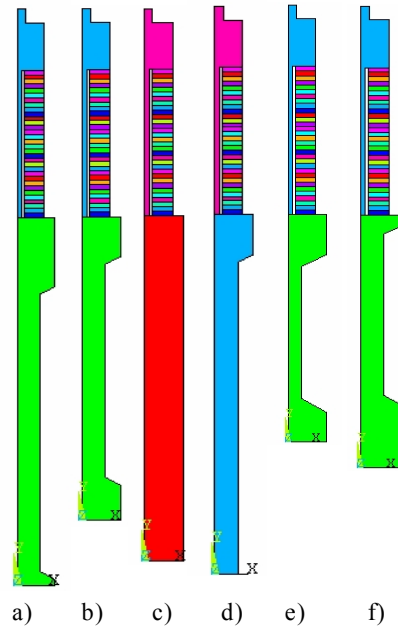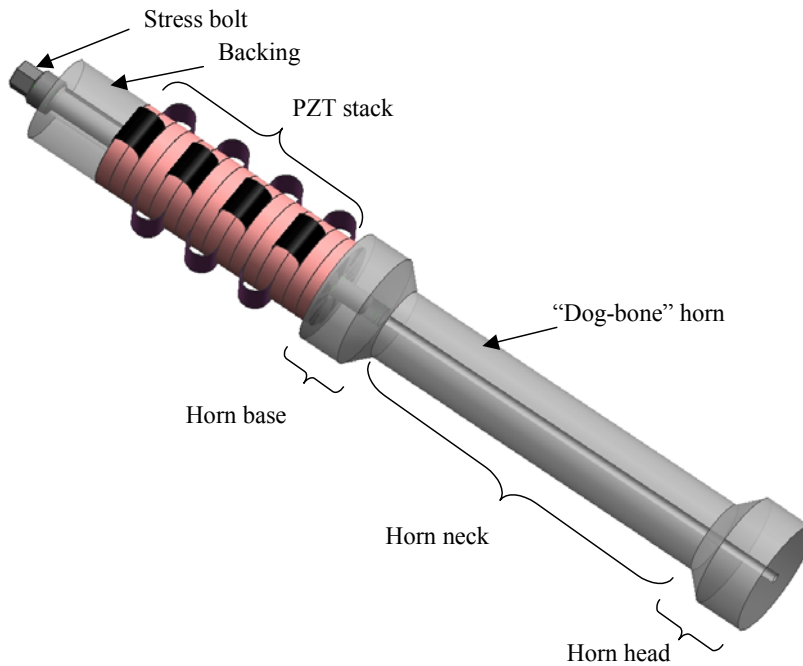
Figure 7 - Analysis designs

Figure 8 - USDC rendering

The designs are shown in Fig. 7 where the stack is represented with the same dimensions and the relative lengths of the horns can be compared. For all these designs various dimensions free-masses were analyzed and the total power transmitted to the bit stem was plotted in Fig. 9. It can be seen that the best performance is obtained for the design having a thin neck (Fig. 7,e), while using a 250g free mass. It should be noted that other design criteria might give a different best performer. One of these criteria could be the efficiency or the total energy transferred to the bit stem by impacts having a linear momentum greater than threshold.
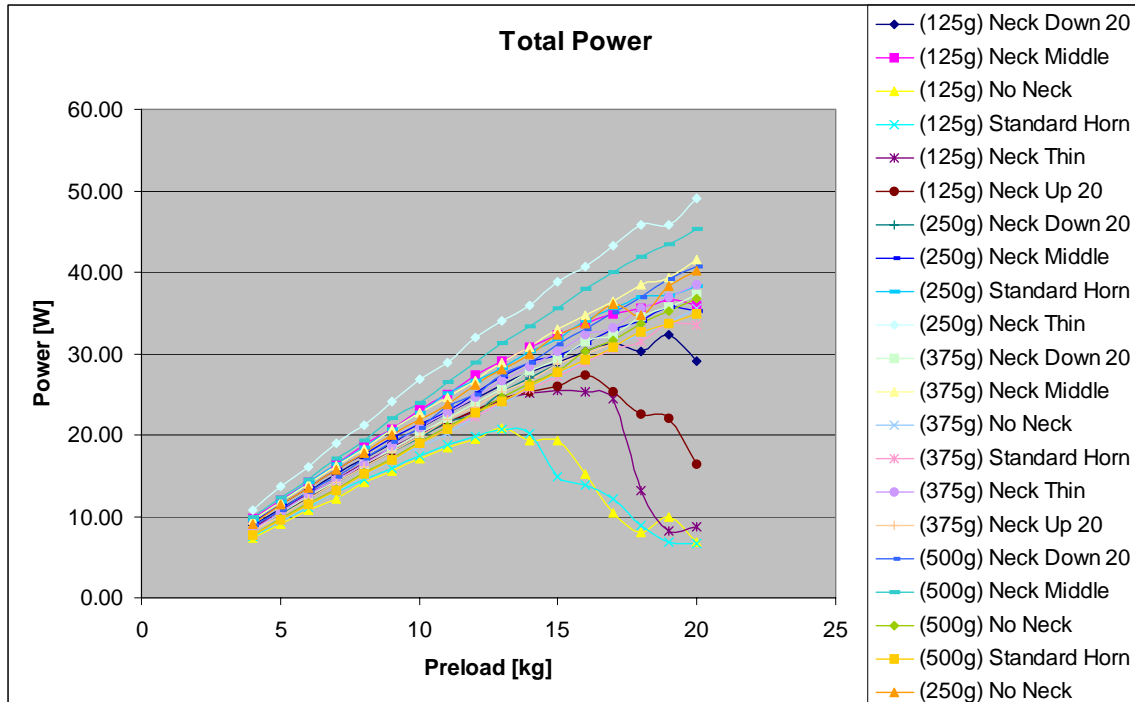
Figure 9 - Total power output

5. CONCLUSION

The routines that perform the analysis of the USDC have been integrated in a program package that can run automatically requiring less human intervention. This program package used in the analysis of the application of the USDC for an ice drill and the analysis results were presented in this paper. The running time of the whole package has been reduced from a period of time ranging from a few days to a week with human supervision to 8-15 hours without human intervention. The program package can now be modified to include a numeric optimal design algorithm, like the Genetic Algorithm, for improved design capabilities.

REFERENCES

1. Bar-Cohen, Y., Sherrit, S., Dolgin, B., Bao, X., Chang, Z., Krahe, R., Kroh, J., Pal, D., Du, S., Peterson, T., "Ultrasonic/Sonic Driller/Corer(USDC) for planetary application," *Proc. SPIE Smart Structure and Materials 2001*, pp. 529-551, 2001.
2. S. Sherrit, X. Bao, Z. Chang, B. Dolgin, Y. Bar-Cohen, D. Pal, J. Kroh, T. Peterson "Modeling of the ultrasonic/sonic driller/corer: USDC," 2000 IEEE Int. Ultrason. Symp. Proc., vol.1,pp. 691-694, 2000.
3. Bao, X., Bar-Cohen, Y., Chang, Z., Dolgin, B. P., Sherrit, S., Pal, D. S., Du, S., Peterson, T., "Modeling and Computer Simulation of Ultrasonic/Sonic Driller/Corer (USDC)," *IEEE Transactions on Ultrasonics, Ferroelectrics and Frequency Control (UFFC)*, Vol. 50, No. 9, pp. 1147-1160, Sept. 2003.
4. S. Sherrit, B. Dolgin, Y. Bar-Cohen, D. Pal, J. Kroh, T. Peterson, " Modeling of horns for sonic/ultrasonic applications," 1999 IEEE Int. Ultrason. Symp. Proc., pp. 647-651, 1999.
5. H. Allik and T.J.R. Hughes, "Finite Element Method for Piezoelectric Vibration," Int. J. Num. Math. Eng., Vol. 2, pp. 151-157, 1970.
6. Y. Bar-Cohen, S. Sherrit, Z. Chang, L. Wesse, X. Bao, P. T. Doran, C. H. Fritsen, F. Kenig, C. P. McKay, A. Murray, and T. Peterson, "Subsurface Ice and Brine Sampling Using an Ultrasonic/Sonic Gopher for Life Detection and Characterization in the McMurdo Dry Valleys," Proceedings of the SPIE Smart Structures Conference San Diego, CA., SPIE Vol. 5388-32, Mar 14-18, 2004.